Development of a high-resolution real-time-capable 3D SONAR camera for deep sea operation

Michael EHRHARDT, Franz Josef BECKER, Daniel SPEICHER, Heinrich FONFARA, Holger HEWENER, Christian DEGEL, Steffen TRETBAR

Fraunhofer Institute for Biomedical Engineering IBMT
Ensheimer Strasse 48, 66386 St. Ingbert, Germany
Michael.Ehrhardt@ibmt.fraunhofer.de

Within this work we present a first experimental setup of a high-resolution real-time-capable 3D sonar camera system for deep sea operation. Since we are currently in the development process, the focus of this work is on the transmission aspects of the camera. Following publications will include the receiving aspects as well as the first phantom reconstructions. The system consists of a 1024 element matrix array antenna, together with a 128 channel beamforming system including a 1:8 multiplexing device for each channel. The camera is supposed to deliver volumetric images within a range of up to 15 m in a deep sea environment up to 6000 m depth. The antenna provides the advantage of an adjustable defocused transmitting sound field. This allows dynamic control of the field of view, and an increase of the image contrast for a specific region.

Keywords: 2D array, matrix array, 3D imaging, beamforming

1. Introduction

The deep sea, and especially the seafloor, constitute an increasingly attractive field for various scientific and economic interests. In order to accomplish a comprehensive exploration, as well as an efficient economic utilization, of the deep sea, visualization tools which provide images of reasonable quality within an acceptable period of time are required. However, the commonly used optical imaging systems are very restricted in the seafloor area due to the high concentration of suspended matter – especially during ongoing operations – and are therefore insufficient for many applications. Thus, we propose a high-resolution real-time-capable sonar system to overcome the limitations of optical imaging, and ensure an adequate visualization for exploration and process monitoring purposes. Though there are numerous different sonar systems available which are used for imaging purposes, there is no sonar system commercially available to date which is able to provide real-time 3D images with a sufficient spatial resolution in a deep sea environment.

Therefore, this work deals with the development of a sonar camera system which meets the requirements of the applications in the field of deep sea volumetric imaging.

2. Antenna

The acoustic antenna defines the overall performance of the whole camera system. A two-dimensional matrix array of 32 x 32 single transducer elements was chosen to form a combined transmitting and receiving antenna [1]. The antenna is shown in Figure 1.

The advantage of a transmitting aperture consisting of parallel addressable transducer elements is an adjustable sound field. The nominal operation mode of the antenna provides a defocused transmission with a sound opening angle of approximately 35° in azimutal and elevational direction. The defocused transmission is performed by a suitable assignment of excitation delays to the single antenna elements. Using different sets of excitation delays, the antenna's sound field can be constricted (decreased defocusing) or widened (increased defocusing). A wider sound field means a larger field of view per transmission event, and is essential for real-time imaging. However, the sound field can be specifically constricted to a certain region of interest, in order to receive stronger echo signals, leading to a higher image contrast in that region.

The center frequency of 1 MHz consititutes a compromise between a sufficent resolution, and an acceptable propagation loss within sea water. The center-to-center distance between two neighboured transducer elements was chosen to be 2λ (3 mm), which constitutes a compromise between a proper lateral resolution, and an acceptable level of side lobes and grating lobes within the antenna's sound field.

A 1-3 piezo-composite material was chosen to be the active transducer material, due to its advantages in signal amplitudes (higher transmitting and receiving sensitivity) and acoustic bandwith (transmission of shorter signals or frequency coded signals).

The single transducers have been acoustically optimized using a backing material with a low acoustic impedance, and two frontside matching layers. The backing material has been selected to ensure a preferably high sensitivity of the transducers, while the matching layers have been processed in order to increase the acoustic bandwidth primarily.

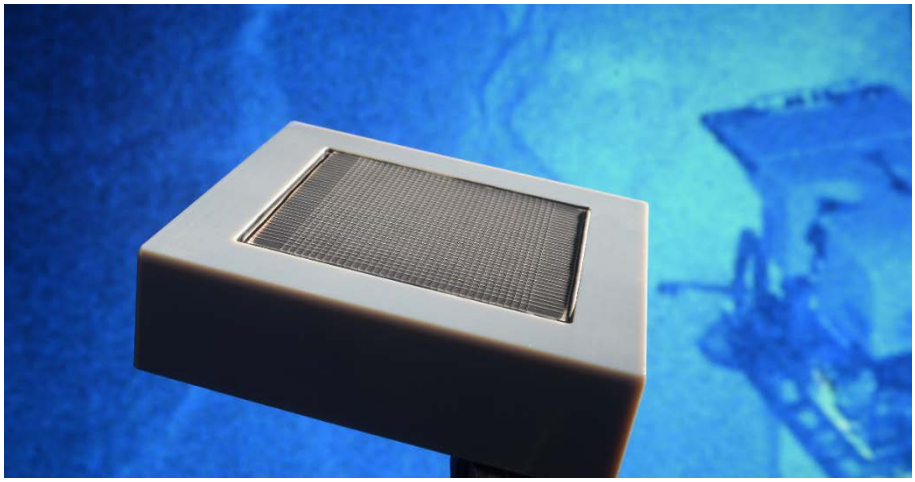

Fig. 1. Aperture with 1024 single transducer elements.

In order to provide sufficient protection against the surrounding sea water, the aperture has been moulded with a special casting compound for sonar applications. This compound

provides, among other qualities, a low water absorption level, an acoustic impedance close to that of water, and a low level of acoustic damping.

The antenna housing is made of anodized aluminium, to ensure resistance against corrosion from saltwater.

For the sake of simplicity, we set up this first prototype in a non-pressure resistant design, since the focus was on the characterization of the antenna´s acoustic and electrical behavior. However, in former projects we investigated a pressure neutral design concept for electronics and transducers [2] which will be transferred to the current prototype to achieve compatibility within a deep sea environment.

Using our pressure chamber, we are able to validate the pressure-resistance of the system up to a value of 600 bar, and even perform functional tests under pressure.

The single antenna elements have been randomly measured in order to determine their electrical and acoustic performance and uniformity.

The electrical impedances of the transducer elements have been measured using a network analyzer. The measurements have been performed with the elements directly connected to the analyzer without the connecting cables in between. The impedance curves can be found in Figure 2.

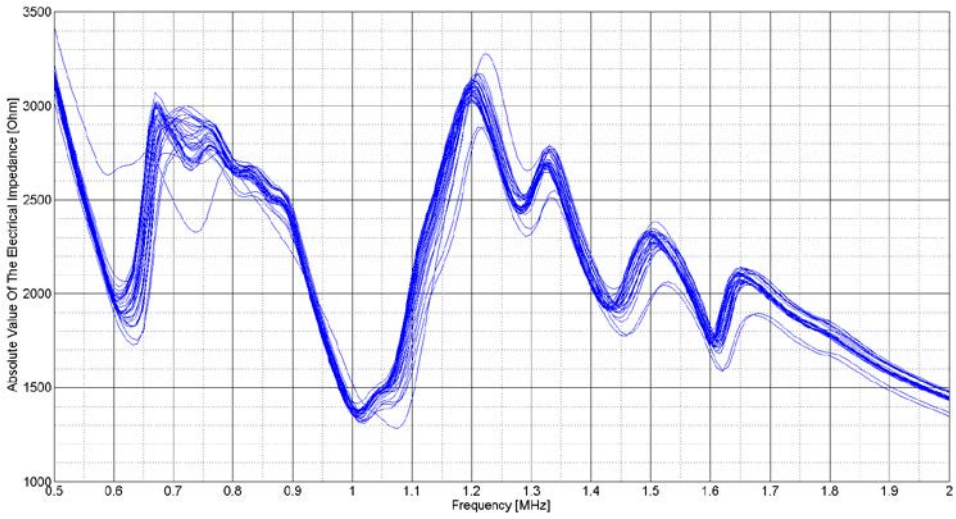

Fig. 2. Electrical impedances of randomly measured antenna elements.

The plots show a quite even and homogenous progression of the impedance over the frequency. However, it becomes obvious that the impedance level is relatively high. In transmission mode, groups of 8 transducer elements are connected to one beamformer channel, so that the electrical impedance of the load decreases to an eighth. Nevertheless, an electrical matching between the antenna and the beamformer system would provide a further improvement of the signal amplitudes, and is currently being investigated.

The acoustic performance has been measured in pulse-echo mode against a plain steel reflector at a distance of 30 cm. A pulser/receiver device has been used to perform these measurements. Figure 3 shows a recorded echo signal, while Figures 4 to 6 show the distributions of the measured values for the signal amplitudes, the acoustic center frequencies, as well as the acoustic bandwidths of the single antenna elements.

Fig. 3. Waveform of the pulse-echo measurement of a single antenna transducer element.

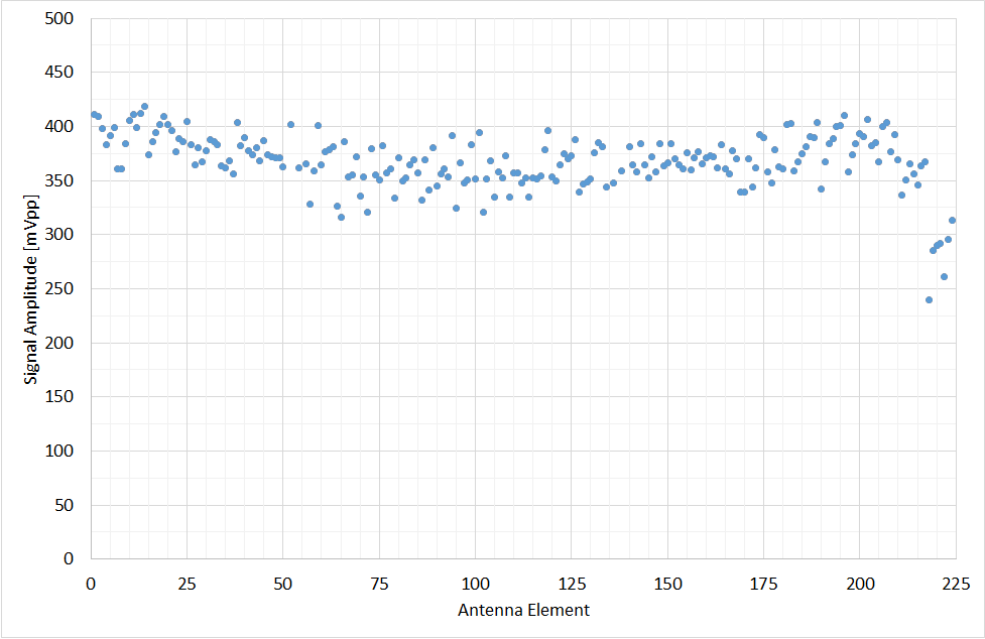

Fig. 4. Signal amplitude of randomly measured antenna elements.

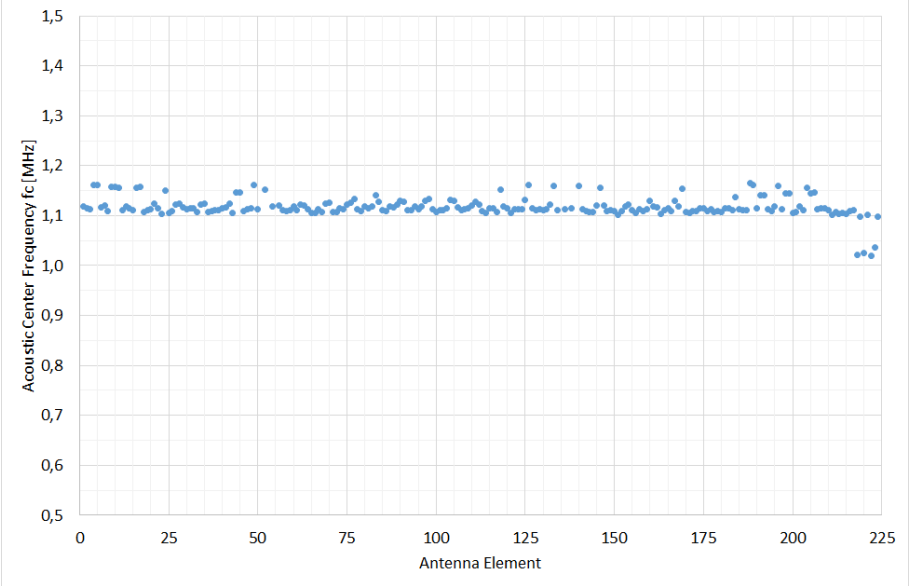

Fig. 5. Acoustic center frequency of randomly measured antenna elements

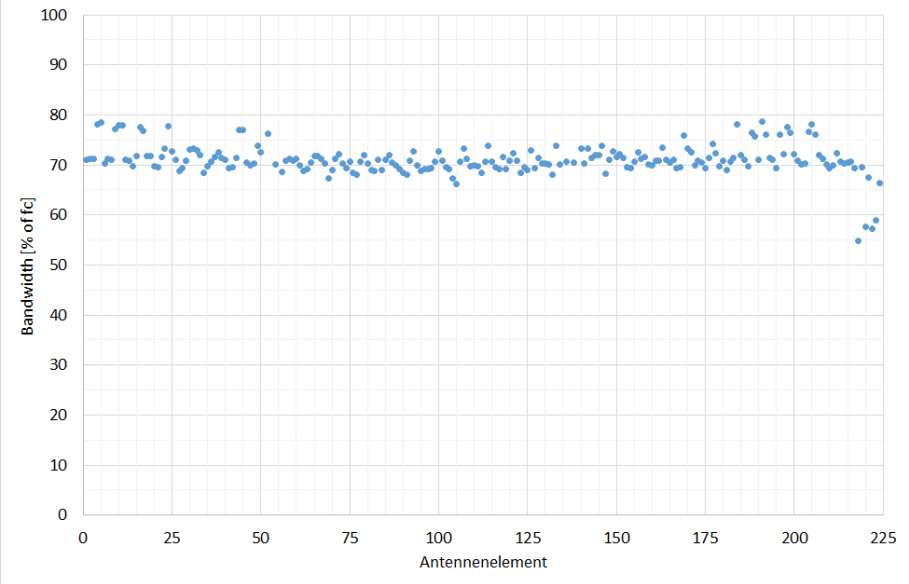

Fig. 6. Acoustic bandwidth of randomly measured antenna elements in percentage of the center frequency.

The statistical results for the acoustic measurements can be found in the following table.

Tab. 1. Statistical results of the acoustic performance of the antenna transducer elements.

	Signal Amplitude	Center Frequency fc	Bandwidth
Mean Value	367 mVpp	1.12 MHz	71 % of fc
Standard Deviation	26 mVpp	20 kHz	3 % of fc

In order to investigate the cross-talk level between neighboured antenna elements, a measurement with a laser vibrometer has been performed. In this measurement one transducer element was electrically excited with a long sinusodial signal and the surrounding surface displacement has been scanned to evaluate the mechanical cross-coupling. If the cross-coupling between the transducer elements is too high, the image quality will be reduced. The scanning grid was 600 µm in x and y direction. The average surface displacement of the aperturę, for the duration of the measurement, can be found in Figure 7.

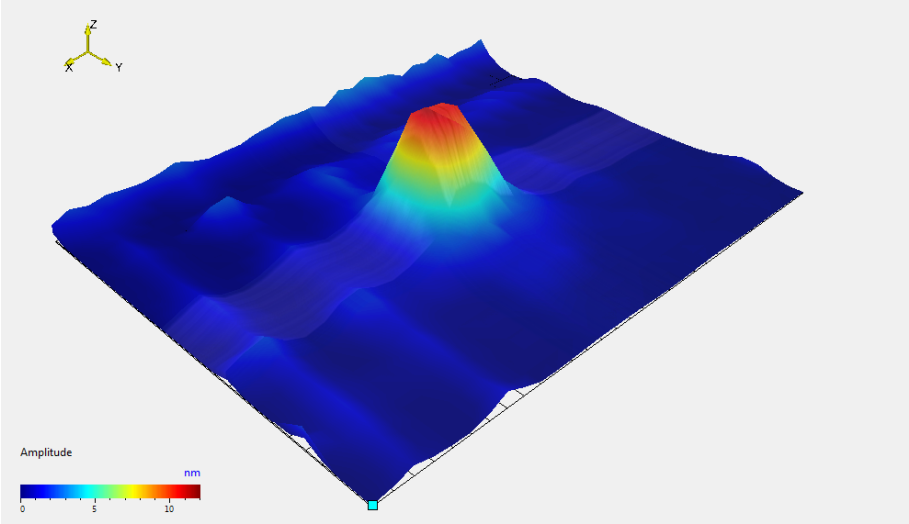

Fig. 7. Laser vibrometer displacement measurement of the aperture.

The cross-talk level between neighboured elements was calculated to approximately -20 dB, which is an appropriate value in order to achieve a sufficient image quality. Figure 8 shows a picture of the antenna in a housing of anodized aluminium, with connecting cables of 2 m length.

Fig. 8. 3D sonar camera with connecting cables of 2 m length.

3. Beamformer system

The generation of the electrical excitation signals, the delayed excitation of the single transducer elements, as well as the receiving of the echo signals, and the processing for the image reconstruction is performed by an electronic FPGA based beamformer system [3]. This sonar beamformer provides 128 parallel channels combined with a 1:8 multiplexing for each channel. With this setup the 1024 transducer elements can be controlled in transmitting and receiving. The system provides a digitalization rate of 40 MHz, and is able to handle transducers with a center frequency of up to 10 MHz. Figure 9 shows a functional overview.

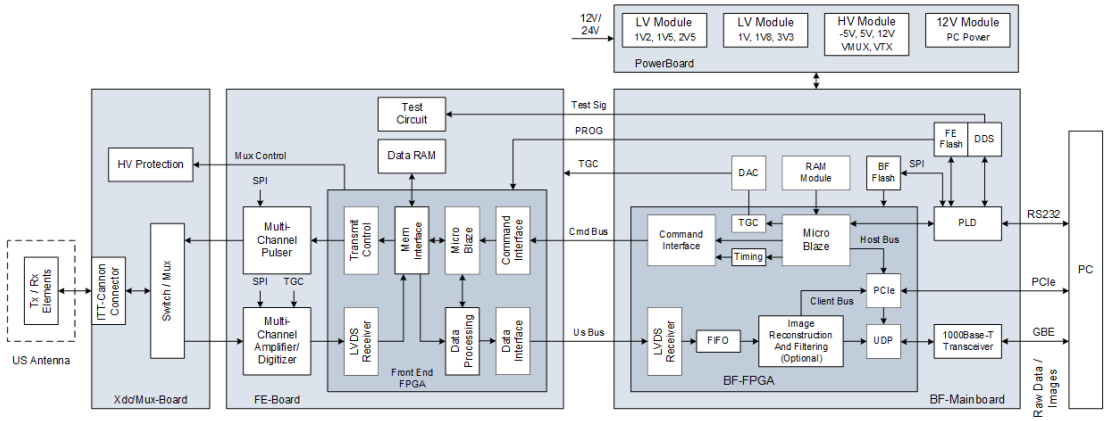

Fig. 9. Functional overview of the sonar beamformer system.

The beamformer allows the excitation of arbitrary tri-state signals with amplitudes up to ±75 V, which can be programmed using bit patterns with a resolution of 8.3 ns (Figure 10). These patterns can be specified for each channel individually. Based on this, frequency coded signals can be generated, and used for excitation. These signals can be used for matched filtering during the image reconstruction, which increases the SNR and offers the opportunity to use longer transmission signals without decreasing the axial resolution.

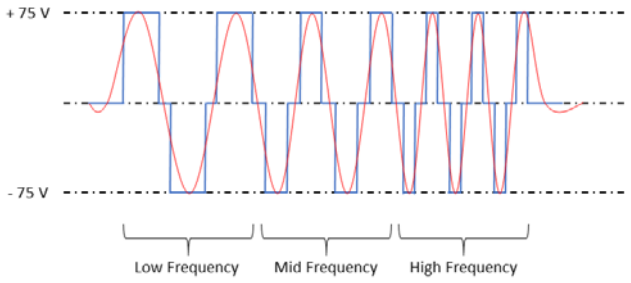

Fig. 10. Generation of frequency coded signals with the beamformer system using bit patterns.

Regarding the receiving path of the beamformer, full data access is available at any stage of the signal processing chain. Direct real-time image reconstruction and filtering, as well as raw data output for later-on offline reconstruction and filtering, is provided.

The usage of 1:8 multiplexing for each channel makes it necessary to combine the transducer elements in groups of 8 for the transmission of a defocused sound field.

For a transmission event, each multiplexer connects all 8 plugged transducer elements and excites them at the same assigned delay time. This leads to circular element arrangements

for the single transmission delays. For defocused transmission, the 128 circular transducer groups are excited, beginning from the center of the aperture to its margins (Figure 11).

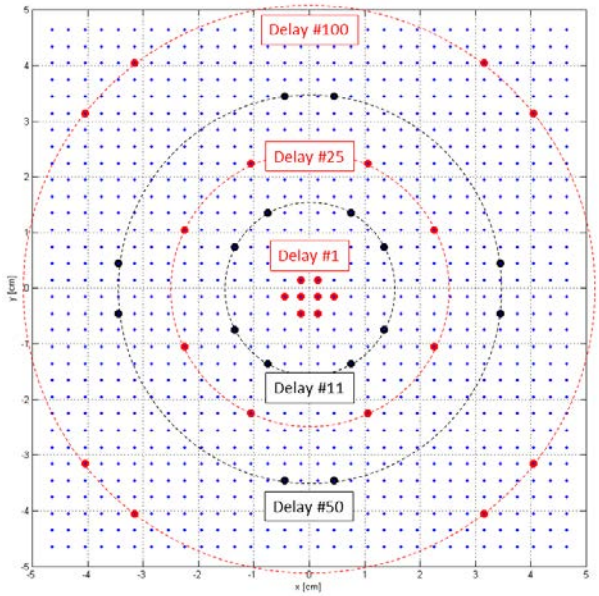

Fig. 11. Schematic illustration of the transmit delay distribution of the single antenna elements for defocused transmission. The dots represent the single transducer elements. 128 delays are used for one transmission event.

After the complete excitation of all 128 channels, and their connected transducer elements, the multiplexers switch to receive mode. Now, only one element per multiplexer is connected to the receive path of the beamformer system. Accordingly, in order to process the received echo signals from all 1024 elements, 8 transmitting and receiving events are necessary. However, with only one transmitting and receiving event the signal data of 128 elements is available, and can be used for image reconstruction. With every following event the reconstructed image becomes more accurate. So, depending on the requirements of the application, it is not always necessary to perform all 8 transmitting/receiving events in order to get an adequate image of the surrounding environment.

4. Sound field measurements

The experimental setup of the camera system has been used in order to measure different sound pressure distributions resulting from different excitation delay sets for the antenna elements. The nominal operation mode provides a sound opening angle of approximately 35° x 35° at -3 dB.

Two additional delay sets have been used to investigate the sound pressure fields using a less defocusing, and a more defocusing, excitation of the antenna (Figure 12).

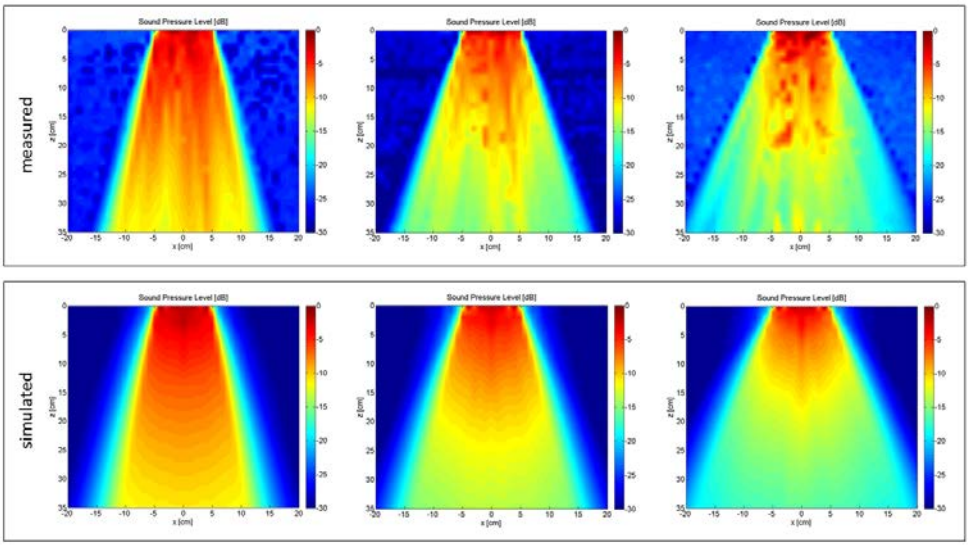

Fig. 12. Sound pressure fields of the antenna using different grades of defocusing. Nominal defocusing (mid), decreased defocusing (left), increased defocusing (right).

It can be seen that the sound fields widen up from left to right in accordance with the simulation results below. Furthermore, it becomes obvious that the sound fields become more inhomogenous with increased defocusing.
The measurements of the sound fields in a parallel plane at 30 cm distance from the aperture show similar results (Figure 13).

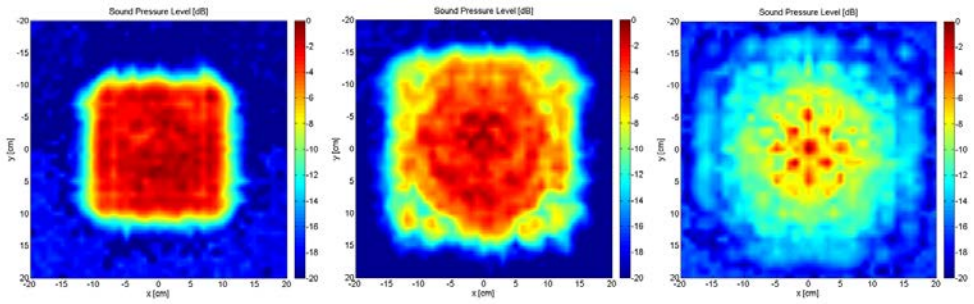

Fig. 13. Sound pressure distributions in a parallel plane at 30 cm distance from the aperture using different grades of defocusing. Nominal defocusing (mid), decreased defocusing (left), increased defocusing (right).

The sound opening angle increases, but the sound pressure distribution becomes more inhomogenous with higher grades of defocusing.

5. Conclusion

We have presented a first setup of a 3D sonar camera which is supposed to provide high-resolution volumetric images in real-time at distances up to 15 m. Sound field measurements have been performed in order to prove the concept of defocused transmission with an adjustable sound opening angle. This feature provides the opportunity of an adjustable field of view, and image contrast.

The electrical and acoustic characterization of the antenna shows that the single transducers offer an appropriate performance for the proposed application. The electro-

acoustic properties of the antenna elements are quite homogenous, and the cross-talk level between the elements is sufficiently low.

The system allows the transmission of frequency-coded signals which can be used for matched filtering algorithms during reconstruction. Together with additional filter algorithms, the image quality can be strongly improved.

Both real-time image reconstruction, as well as raw data output for offline reconstruction, is feasible; with the camera system ensuring a maximmum of flexibility for the operator.

The next steps will involve the reconstruction of various phantoms and real structures in water tanks, as well as the open water environment, to prove the high-resolution and real-time-capability. Different filter algorithms will be developed and implemented, in order to reduce the impact of reconstruction artifacts, and improve the image resolution and quality. The spatial merging of the antenna and the beamformer system, in one compact housing, is another task in order to achieve a flexible and user-friendly device for various applications.

Fig. 14. Experimental setup of the 3D sonar camera system

References

[1] M. Ehrhardt, F. J. Becker, F. Motzki, D. Speicher, C. Degel, Concept For A High-Resolution Real-Time Capable 3D Sonar Camera For Deep Sea Operation, 3rd International Conference and Exhibition on Underwater Acoustics UACE 2015 Platanias, Crete, Greece, 21-26 June 2015.

[2] M. Molitor, M. Moses, M. Schmieger, O. Walter, P. Weber, R. Lemor, A pressure-neutral acoustic transmit receive module (PR-TRM) with integrated data processing for deep sea applications, International Oceans Conference and Exhibition, Sydney, Australia, 24-27 May 2010.

[3] H. J. Hewener, H. J. Welsch, H. Fonfara, F. Motzki, S. H. Tretbar, Highly Scalable and Flexible FPGA Based Platform for Advanced Ultrasound Research, IEEE International Ultrasonics Symposium Proceedings, 2075-2080, 2012.